Catalysis Communications 101 (2017) 120–124

Contents lists available at ScienceDirect

Catalysis Communications

journal homepage: www.elsevier.com/locate/catcom

Short communication

Reaction mechanisms of acetylene hydrochlorination catalyzed by $AuCl_3$/C catalysts: A density functional study

Fanfan Wan[a], Songlin Chao[a], Qingxin Guan[a], Gui-chang Wang[a,**], Wei Li[a,b,*]

[a] College of Chemistry, Key Laboratory of Advanced Energy Materials Chemistry (Ministry of Education), Nankai University, Tianjin 300071, China
[b] Collaborative Innovation Center of Chemical Science and Engineering, Tianjin 300071, China

A B S T R A C T

Reaction mechanisms of acetylene hydrochlorination catalyzed by $AuCl_3$/C catalysts were investigated by density functional theory calculations. Tri-coordinated gold chloride with a vacant site shows high activity in adsorbing HCl and C_2H_2. Mechanisms in the first adsorption of HCl and C_2H_2 on gold were found to be the Eley-Rideal (ER) and the Langmuir-Hinshelwood (LH) mechanisms, respectively. The transfer of Cl atom of $AuCl_3$ to acetylene is the key step in the LH mechanism, which could form new vacant site to adsorb HCl effectively. Tri-coordinated gold was formed by removing Cl atom through addition reaction of acetylene in the induction period.

1. Introduction

Polyvinyl chloride (PVC) is the world's third best-selling polymer. Vinyl chloride monomer (VCM), the monomer of PVC, is a significant commodity chemical with a production over 40 million tons annually [1]. Owing to abundant and inexpensive coal resource, over 13 million tons of VCM is produced annually in China by acetylene hydrochlorination using the $HgCl_2$/C catalysts [2,3]. Due to the great harm to environment and human health of mercury, it is very urgent to develop non-mercury catalysts for PVC production. Among the non-mercury catalysts, supported gold catalysts have great potential as industrial catalysts [1,4].

Surface functional groups of activated carbon play a significant role in $AuCl_3$/C catalysts [5]. Our group found that ketone, lactone and/or carbonyl tend to improve the activity of catalysts [6]. Hutchings et al. performed pioneering theoretical calculations for the reaction mechanism using model of $AuCl_3$ molecule and speculated that $AuCl_3$ inclines to adsorb C_2H_2 on the vacant site first and then HCl is introduced via a HCl-HC hydrogen bond [7]. Zhang et al. proposed reaction mechanisms using model of Au_2Cl_6 where the complex of HCl and C_2H_2 would be adsorbed [8]. Recently, Hutchings et al. made a significant breakthrough published in *Science* on identification of active sites of $AuCl_3$/AC catalysts under reaction conditions [9]. They perfectly proved that highly active catalysts comprise single-site cationic Au entities whose result of EXAFS fitting a first coordination shell for Au-Cl gave an average coordination number of 2.6. Despite the splendid research that has been reported, the reaction mechanism of acetylene hydrochlorination catalyzed by $AuCl_3$/AC has not yet been determined experimentally. And the adsorption of HCl is weak in previous theoretical study [7,8], which makes it hard to carry out the reaction.

In this work, we first investigated interactions between $AuCl_3$ and oxygen-containing functional groups and adsorption strength of HCl and C_2H_2 on $AuCl_x$ to determine the model of catalysts. Using this model, we explored the ER and LH mechanisms for acetylene hydrochlorination systematically.

2. Methods

2.1. Calculation details

Periodic plan-wave based DFT calculations were performed using Vienna ab initio simulation package (VASP) [10,11]. The exchange and correlation effects were treated by the generalized gradient approximation (GGA), using the vdW-DF [12] with Perdew–Burke–Ernzerhof (PBE) functional [13] to describe weak interactions. Electron-ion interactions were described by the projector-augmented plane-wave (PAW) method [14,15]. The energy cutoff of 400 eV for the plane-wave basis was used for all calculations. $3 \times 1 \times 1$ Monkhorst-pack [16] mesh was used to calculate the total energy of system, and $9 \times 1 \times 1$ Monkhorst-pack mesh was used to perform electronic analysis. The convergent of energy and forces were set to 1×10^{-4} eV and 0.05 eV/Å.

* Correspondence to: Wei Li, College of Chemistry, Key Laboratory of Advanced Energy Materials Chemistry (Ministry of Education), Nankai University, Tianjin 300071, China.
** Corresponding author.
E-mail addresses: wangguichang@nankai.edu.cn (G.-c. Wang), weili@nankai.edu.cn (W. Li).

http://dx.doi.org/10.1016/j.catcom.2017.07.022
Received 18 April 2017; Received in revised form 25 July 2017; Accepted 25 July 2017
Available online 27 July 2017

The transition state (TS) was determined by three steps: first, we employed the climbing nudged elastic band (cNEB) [17,18] method to get the likely TS; then, we used the quasi-Newton algorithm method to optimize the likely TS by minimizing the forces on each atom until they fell below 0.05 eV/Å; finally, we performed frequency analysis to confirm the TS. Here, the adsorption energy (E_{ads}) and activation energy (E_a) were determined by the following formulas: $E_{ads} = E_{A\text{-}M} - E_A - E_M$ and $E_a = E_{TS} - E_{IS}$, where $E_{A\text{-}M}$, E_A, E_M, E_{TS} and E_{IS} represent the total energy of the adsorbed structure, isolated molecules, substrate, TS and initial state (IS), respectively.

The free energies are calculated by taking account of entropy contributions of HCl and C_2H_2 adsorptions and C_2H_3Cl desorption. The formula is: $S = 1.5R\ \ln(2\pi MkT) - 3R\ \ln h + R\ \ln(kT/P) + 2.5\ R$[19]. The reaction was carried out at 453 K and standard pressures [6]. The adsorptions of HCl and C_2H_2 lose 0.76 eV and 0.74 eV of entropy energies (TS), respectively, and the desorption of C_2H_3Cl gains 0.79 eV. We carried out reaction kinetic analysis of catalytic cycles using energetic span model [20]. A simple estimation of the TOF can be calculated by the approximate formula: TOF $\approx \frac{k_B T}{h} e^{-\delta E/RT}$.

2.2. Calculation models

There are multiple studies using the model of a single layer of graphene with edge atoms to simulate carbonaceous surfaces [21–23]. Hence, we used a single-layer graphene with zigzag C edges saturated by H atoms, consisting of six benzene rings in width and five benzene rings in length (Fig. S1). To prevent the interaction between periodic structures, we set a vacuum region of 15 Å and 10 Å in the perpendicular and parallel direction, respectively. All the atoms in the model are relaxed. The optimized C—C bond length of the central benzene ring is 1.43 Å and 1.42 Å, in accordance with the experimental results of 1.42 Å basically [24].

Studies of surface oxygen-containing functional groups on $AuCl_3$/C catalysts mainly concerned about ether, phenol, ketone and carboxyl groups [5,6,25]. Therefore, to simplify the calculation, we modelled ether, phenol, ketone and carboxyl (Fig. S1). Hutchings et al. have proved that $AuCl_3$/AC catalysts comprise single-site cationic Au entities under acetylene hydrochlorination reaction conditions, [10] proving it reasonable using single $AuCl_3$ to investigate the interaction with oxygen-containing groups, which is formed after adsorption of $AuCl_4^-$ and release of Cl^- [26].

Au atom is located above O atom of ether and phenol, at a distance of 2.87 Å and 3.07 Å (Fig. S2), respectively, indicating that they adsorb $AuCl_3$ weakly. As shown in Fig. 1, adsorption energy of $AuCl_3$ on ketone is − 1.47 eV, and Au—O bond length is 2.16 Å. While for carboxyl, adsorption energy is − 1.89 eV and Au—O bond length is 2.20 Å, longer than that of ketone, pointing out that Au atom interacts a little stronger with O atom of ketone than that of carboxyl. Fig. 1 shows that H—Cl bond length of carboxyl is much shorter than that of ketone, which is the main reason for the higher adsorption energy for carboxyl than ketone. The results of charge density difference of adsorption configurations (Fig. S4) show that O atoms on ketone and carboxyl anchor $AuCl_3$ strongly through *p* bands of O atom and *d* bands of Au atom by covalent effects. We also investigated interactions of $AuCl_3$ with two oxygen-containing groups (Fig. S3), the configurations of gold almost stay the same with single oxygen-containing groups. Hence, we only explored reaction mechanisms on $AuCl_3$ with single oxygen-containing groups.

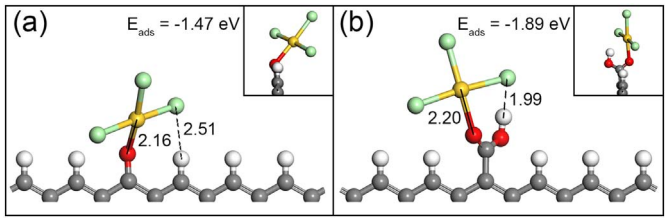

Fig. 1. Adsorption configurations of $AuCl_3$ on (a) ketone and (b) carboxyl of active carbon. All distances in Å. H is white, C is grey, O is red, Cl is green and Au is yellow. (For interpretation of the references to colour in this figure legend, the reader is referred to the web version of this article.)

3. Results and discussion

As for $AuCl_3$ on carboxyl (Fig. S5), the adsorption energy for HCl is 0.28 eV, and C_2H_2 is introduced weakly through σ-π interaction on HCl with adsorption energy of − 0.25 eV. The reaction barrier of TS is 1.09 eV. However, the configuration of gold catalyst cannot be restored after reaction. The reaction mechanism on ketone (Fig. S6) is similar with carboxyl. Thus, we only explore reaction mechanisms on carboxyl here. Besides, the adsorption of C_2H_2 firstly on $AuCl_3$ makes it difficult to adsorb HCl successively. The results suggested that it is hard for tetra-coordinated gold to catalyze acetylene hydrochlorination.

It is well known that typically crystals of gold chloride are $AuCl_3$ with square tetra-coordinated Au and AuCl with linear bi-coordinated Au, indicating tetra-coordinated and bi-coordinated gold is very stable. We investigated adsorption strength of HCl and C_2H_2 on $AuCl_x$ (x = 1–4) molecules (see Fig. S7), and found that bi-coordinated and tetra-coordinated gold interacts weakly with HCl and C_2H_2, while single coordinated and tri-coordinated gold interacts strongly with reactants. The results are in agreement with Hutchings' theoretical studies that $AuCl_3$ molecule could adsorb HCl and C_2H_2 strongly. Single coordinated gold adsorbs C_2H_2 too strongly with adsorption energy of − 1.72 eV, making it hard to continue the reaction. The adsorption energy for HCl and C_2H_2 on single $AuCl_3$ is − 0.79 eV and − 1.10 eV, respectively, suggesting Au(III) with a vacant site could adsorb reactants properly. The conclusion is consistent with the previous study that active sites of K_2PdCl_4 catalysts are Pd (II) chloro complexes with a coordination vacancy, capable of reversibly forming π-acetylene complexes [27]. The formation mechanism of tri-coordinated gold will be discussed in Section 3.3. Here, we explored reaction mechanism of acetylene hydrochlorination on Au(III) with a vacant site.

3.1. The ER mechanism of acetylene hydrochlorination

The ER mechanism in the first adsorption of HCl is shown in Fig. 2. Here, we take the calculated energies of gold catalyst, C_2H_2 and HCl as arbitrary zero. Adsorption energy of HCl is − 0.39 eV. Bader charge analysis [28] (Fig. S8) shows that the positive charge (+ 0.78 e) of Au

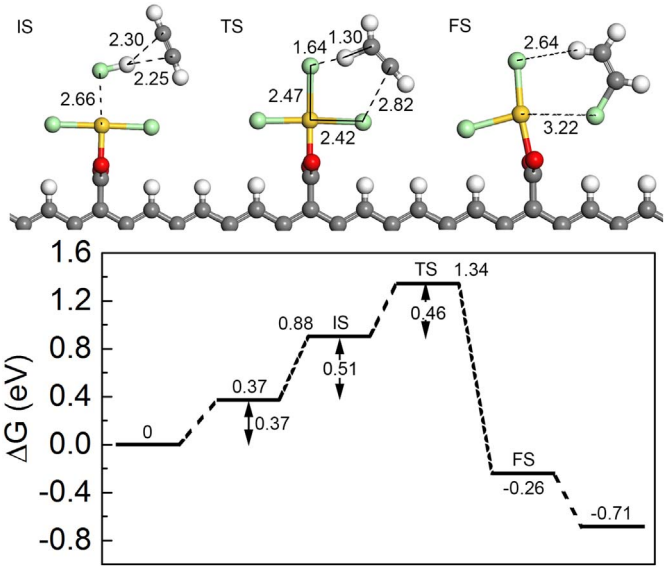

Fig. 2. The ER mechanism for acetylene hydrochlorination.

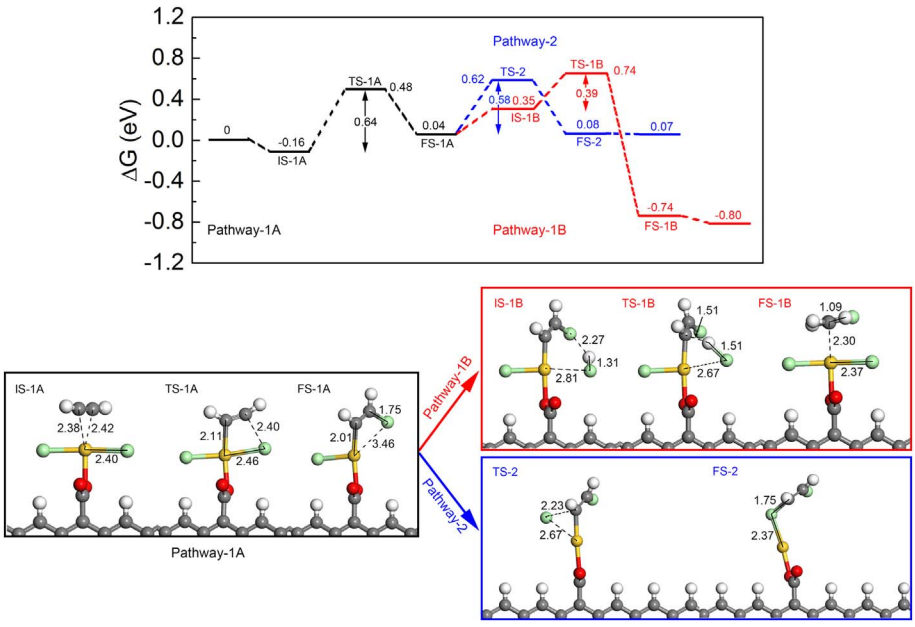

Fig. 3. The LH mechanism and deactivation mechanisms for acetylene hydrochlorination.

(III) with a vacant site is less than that (+ 0.83 e) of Au(III), suggesting electrostatic interaction is not the main effect between HCl and Au(III) with a vacant site. C_2H_2 is adsorbed through σ-π interaction on HCl with adsorption energy of − 0.24 eV, distances between H and C atoms are 2.30 Å and 2.25 Å. In TS, there is a six-membered ring consisted of HCl, C_2H_2 and $AuCl_2$. The H−Cl bond of HCl is strongly stretched by 0.35 Å, and H atom of HCl is bonded to C atom of C_2H_2 with bond length of 1.30 Å, Cl atom of HCl is attached to Au atom with bond length of 2.47 Å. The Au−Cl bond is slightly stretch by 0.02 Å, and the distance between Cl and C is shortened to 2.82 Å. The reaction barrier to TS is only 0.46 eV, much lower than − 1.09 eV of Fig. S5. The result is attributed to the formation of Au−Cl bond in TS, providing the energy to break H−Cl bond, which cannot happen in TS of tetra-coordinated gold because of no vacant site. The energetic span of the ER mechanism is 1.34 eV with TOF of 0.0116 s^{-1}. The Cl atom in C_2H_3Cl is not from HCl but $AuCl_2$, in which Cl atom is restored from HCl, resulting in the different configuration of $AuCl_2$ from IS. Even though, reaction could carry out on the vacant site of $AuCl_2$ in FS continually.

3.2. The LH and deactivation mechanisms of acetylene hydrochlorination

As shown in Fig. 3, the LH mechanism is consisted with Pathway-1A and Pathway-1B, whereas deactivation mechanism is made up of Pathway-1A and Pathway-2. The adsorption energy of C_2H_2 is − 0.90 eV. After adsorption of acetylene, σ-π interaction and hydrogen bond of HCl were investigated, but the results show that it is difficult to adsorb HCl directly (Fig. S9). Thus, we proposed a novel pathway that one Cl atom on gold transfer to one C atom of C_2H_2. The reaction barrier is 0.64 eV, though it is slight endothermic by 0.04 eV. That indicates the transfer of Cl is possible to carry out. In TS-1A of Pathway-1A, a four-membered ring is formed, one C atom is attached closer to the Au at distance of 2.11 Å, and the distance of C−Cl is shortened to 2.40 Å with the Au−Cl bond stretched by 0.06 Å.

As we can see, there comes a new vacant coordination site in FS-1A, which is very essential to adsorb HCl successively. The adsorption energies of C_2H_2 on FS-1A is − 0.67 eV, much higher than − 0.90 eV of IS-1A because of steric hindrance. While adsorption energy of HCl is − 0.45 eV, lower than − 0.39 eV in Section 3.1 because of H−Cl hydrogen bond. After the adsorption of C_2H_2 in IS-1A, the amount of HCl is more than C_2H_2, giving more chances to adsorb HCl on FS-1A. The result could also explain why there should be more HCl than C_2H_2 in the initial gas. The reaction barrier of Pathway-1B is only 0.39 eV, and it is intensely exothermic by − 0.84 eV, which indicates it is extremely easy to happen. In IS-1B, Cl atom of HCl is adsorbed on Au at a distance of 2.81 Å, and H atom of HCl is located on Cl with a hydrogen bond of 2.27 Å. There is also a four-membered ring in TS-1B, H−Cl bond of HCl is stretched by 0.22 Å, H−C length is shortened to 1.51 Å, and Au−Cl length is 2.67 Å. In the LH mechanism, the energetic span is 0.90 eV with TOF of 915 s^{-1}. The higher value of TOF indicate the LH mechanism is much easier to happen than the ER mechanism.

The transfer of another Cl atom of Au(III) with a vacant site is also evaluated, which is likely the reason for the deactivation of gold catalyst. As shown in Fig. 3, Pathway-2 is slightly endothermic by 0.07 eV, with a reaction barrier of 0.58 eV. In TS-2, the Au−Cl bond is stretched by 0.22 Å with Cl−C at a distance of 2.23 Å. $C_2H_2Cl_2$ is adsorbed strongly on Au by Cl atom with Au−Cl bond of 2.37 Å. After desorption of $C_2H_2Cl_2$, there comes Au(I) with a vacant site, which adsorbs C_2H_2 strongly with adsorption energy of − 1.49 eV. The strong adsorption could prohibit acetylene hydrochlorination to carry on, resulting in deactivation of gold catalysts. Due to the lower reaction barrier and intensely exothermic energy of Pathway-1B, it is not easy for Pathway-2 to happen. The results account for the relatively stability of gold catalysts for acetylene hydrochlorination.

The mechanisms proposed here result in *syn*-addition of HCl to acetylene, in disagreement with result of anti-addition experimentally [7]. In contrast with the experiment in which hex-1-yne and DCl was used, the product was formed by *syn*-addition of HCl to D-hex-1-yne [7]. Thus, further experimental research is needed to evaluate the selectivity of hydrochlorination deeply. In addition, we performed calculations about anti-addition of HCl to acetylene (Fig. S10). The energy barrier of Cl-transfer is 1.71 eV, much higher than 0.64 eV of syn-addition, indicating it is very difficult for anti-addition of HCl to happen.

3.3. Reasonable mechanism to form gold catalyst with a vacant site

There is no calcination in the preparation of catalysts and the temperature of drying is only 403 K [6], indicating that it is difficult to form gold catalysts with a vacant site in the progress of preparation. Here, we proposed a reasonable mechanism for the forming of gold catalyst with a vacant site in Fig. 4. The introduction of C_2H_2 results in adsorption energy of − 0.27 eV. The reaction is exothermic by − 0.29 eV, with a reaction barrier of 1.21 eV, indicating the activation is a little difficult. According to the approximate formula between activation energy and temperature for the first order desorption process at

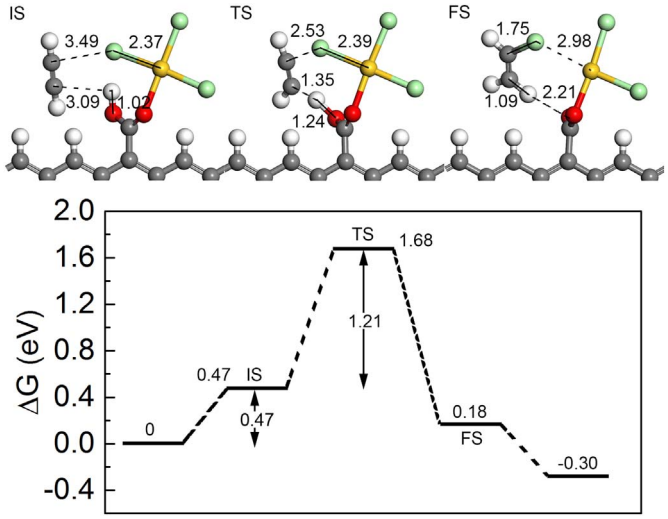

Fig. 4. The mechanism for the formation of $AuCl_2$ with a vacant site.

the near saturation coverage, $E_a = 0.002599 \times T$ (K) [29,30], the estimated energy is 1.18 eV at the temperature of reaction (453 K), which is in agreement with the calculated energy. C_2H_2 is adsorbed to H of carboxyl and Cl of $AuCl_3$ at a distance of 3.09 Å and 3.49 Å, respectively. In TS, there comes a six-membered ring, Au−Cl bond is stretched by 0.02 Å and O−H bond is stretched by 0.22 Å. The desorption energy of C_2H_3Cl is only 0.40 eV. Thus, the activation step is the rate determine step. The configuration of tri-coordinated gold in FS could be transformed into that of IS-1A in Fig. 3, whose calculated energy is slightly lower than that of FS.

Acetylene plays significant role in the induction period, which seems contradictious with common sense that HCl leads to enhanced activity, whereas C_2H_2 causes deactivation [8]. We should make it clear that acetylene definitely benefits for the forming of active sites, but excess of that will lead to deactivation, as discussed in Section 3.2. Thus, HCl needs to be fed immediately after the production of active sites.

4. Conclusions

Here, we investigated reaction mechanisms of acetylene hydrochlorination catalyzed by $AuCl_3$/C catalysts by theoretical calculations. The oxygen species of ketone and carbonyl play important role in stabilizing $AuCl_3$, but the role of these oxygen species during the reaction need to be investigated in future. The calculations indicated Au(III) with a vacant site could catalyze the reaction properly. We proposed a reasonable mechanism for forming Au(III) with a vacant site, in agreement with experimental results that the coordination number of gold in $AuCl_3$/C-AR decreases during the induction period [9]. Both the ER and LH mechanisms are possible pathways in the reaction, but much higher value of TOF for the LH than the ER mechanism indicates the LH mechanism is the dominant mechanism. Transfer of Cl atom of gold chloride is the key step of the LH mechanism, which forms a new vacant site to adsorb HCl effectively. However, transfer of another Cl atom leads to deactivation, which is much more difficult to carry out comparing with the LH mechanism. During the reaction, the coordination number of gold does not change in ER and LH mechanisms and bader charge (Fig. S8) of gold almost stays the same, indicating valence state of gold remains unchanged. The coordination number of gold is three in mechanisms, which is close to 2.6 obtained by recent Hutchings' work [9]. Our results give insights into understanding the catalytic activity of $AuCl_3$/C catalysts and other supported metal complexes catalysts, whose catalytic mechanisms generally could not be determined experimentally.

Acknowledgements

This work was financially supported by the NSFC (21376123, U1403293, 21603107), MOE (IRT-13R30 and 113016A), NSFT (15JCQNJC05500 , 16YFZCGX00020), and the Research Fund for 111 Project (B12015).

Appendix A. Supplementary data

Supplementary data to this article can be found online at http://dx.doi.org/10.1016/j.catcom.2017.07.022.

References

[1] P. Johnston, N. Carthey, G.J. Hutchings, Discovery, development, and commercialization of gold catalysts for acetylene hydrochlorination, J. Am. Chem. Soc. 137 (2015) 14548–14557.
[2] K. Zhou, J. Jia, X. Li, X. Pang, C. Li, J. Zhou, G. Luo, F. Wei, Continuous vinyl chloride monomer production by acetylene hydrochlorination on Hg-free bismuth catalyst: from lab-scale catalyst characterization, catalytic evaluation to a pilot-scale trial by circulating regeneration in coupled fluidized beds, Fuel Process. Technol. 108 (2013) 12–18.
[3] X.-K. Li, Z.-R. Chu, Y.-J. Liu, M.-T. Zhu, L. Yang, J. Zhang, Molecular characterization of microbial populations in full-scale biofilters treating iron, manganese and ammonia containing groundwater in Harbin, China, Bioresour. Technol. 147 (2013) 234–239.
[4] M. Zhu, Q. Wang, K. Chen, Y. Wang, C. Huang, H. Dai, F. Yu, L. Kang, B. Dai, Development of a heterogeneous non-mercury catalyst for acetylene hydrochlorination, ACS Catal. 5 (2015) 5306–5316.
[5] J. Xu, J. Zhao, J. Xu, T. Zhang, X. Li, X. Di, J. Ni, J. Wang, J. Cen, Influence of surface chemistry of activated carbon on the activity of gold/activated carbon catalyst in acetylene hydrochlorination, Ind. Eng. Chem. Res. 53 (2014) 14272–14281.
[6] S. Chao, Q. Guan, W. Li, Study of the active site for acetylene hydrochlorination in $AuCl_3$/C catalysts, J. Catal. 330 (2015) 273–279.
[7] M. Conte, A.F. Carley, C. Heirene, D.J. Willock, P. Johnston, A.A. Herzing, C.J. Kiely, G.J. Hutchings, Hydrochlorination of acetylene using a supported gold catalyst: a study of the reaction mechanism, J. Catal. 250 (2007) 231–239.
[8] J. Zhang, Z. He, W. Li, Y. Han, Deactivation mechanism of $AuCl_3$ catalyst in acetylene hydrochlorination reaction: a DFT study, RSC Adv. 2 (2012) 4814–4821.
[9] G. Malta, S.A. Kondrat, S.J. Freakley, C.J. Davies, L. Lu, S. Dawson, A. Thetford, E.K. Gibson, D.J. Morgan, W. Jones, P.P. Wells, P. Johnston, C.R.A. Catlow, C.J. Kiely, G.J. Hutchings, Identification of single-site gold catalysis in acetylene hydrochlorination, Science 355 (2017) 1399–1403.
[10] G. Kresse, J. Furthmüller, Efficiency of ab-initio total energy calculations for metals and semiconductors using a plane-wave basis set, Comput. Mater. Sci. 6 (1996) 15–50.
[11] G. Kresse, J. Furthmüller, Efficient iterative schemes for ab initio total-energy calculations using a plane-wave basis set, Phys. Rev. B 54 (1996) 11169–11186.
[12] J. Klimeš, D.R. Bowler, A. Michaelides, Van der Waals density functionals applied to solids, Phys. Rev. B 83 (2011) 195131.
[13] J.P. Perdew, Y. Wang, Accurate and simple analytic representation of the electron-gas correlation energy, Phys. Rev. B 45 (1992) 13244–13249.
[14] P.E. Blöchl, Projector augmented-wave method, Phys. Rev. B 50 (1994) 17953–17979.
[15] G. Kresse, D. Joubert, From ultrasoft pseudopotentials to the projector augmented-wave method, Phys. Rev. B 59 (1999) 1758–1775.
[16] H.J. Monkhorst, J.D. Pack, Special points for Brillouin-zone integrations, Phys. Rev. B 13 (1976) 5188–5192.
[17] G. Henkelman, B.P. Uberuaga, H. Jónsson, A climbing image nudged elastic band method for finding saddle points and minimum energy paths, J. Chem. Phys. 113 (2000) 9901–9904.
[18] G. Henkelman, H. Jónsson, Improved tangent estimate in the nudged elastic band method for finding minimum energy paths and saddle points, J. Chem. Phys. 113 (2000) 9978–9985.
[19] Gu X-K, B. Liu, J. Greeley, First-principles study of structure sensitivity of ethylene glycol conversion on platinum, ACS Catal. 5 (4) (2015) 2623–2631.
[20] S. Kozuch, S. Shaik, How to conceptualize catalytic cycles? The energetic span model, Acc. Chem. Res. 44 (2011) 101–110.
[21] L.R. Radovic, B. Bockrath, On the chemical nature of graphene edges: origin of stability and potential for magnetism in carbon materials, J. Am. Chem. Soc. 127 (2005) 5917–5927.
[22] B. Padak, J. Wilcox, Understanding mercury binding on activated carbon, Carbon 47 (2009) 2855–2864.
[23] X. Li, X. Pan, L. Yu, P. Ren, X. Wu, L. Sun, F. Jiao, X. Bao, Silicon carbide-derived carbon nanocomposite as a substitute for mercury in the catalytic hydrochlorination of acetylene, Nat. Commun. 5 (2014).
[24] J. Wilcox, E. Sasmaz, A. Kirchofer, S.S. Lee, Heterogeneous mercury reaction chemistry on activated carbon, J. Air Waste Manage. Assoc. 61 (2011) 418–426.
[25] X. Liu, M. Conte, D. Elias, L. Lu, D.J. Morgan, S.J. Freakley, P. Johnston, C.J. Kiely, G.J. Hutchings, Investigation of the active species in the carbon-supported gold

catalyst for acetylene hydrochlorination, Catal. Sci. Technol. (2016).
[26] U. Becker, M.F. Hochella Jr., D.J. Vaughan, The adsorption of gold to galena surfaces: calculation of adsorption/reduction energies, reaction mechanisms, XPS spectra, and STM images, Geochim. Cosmochim. Acta 61 (1997) 3565–3585.
[27] T.V. Krasnyakova, I.V. Zhikharev, R.S. Mitchenko, V.I. Burkhovetski, A.M. Korduban, T.V. Kryshchuk, S.A. Mitchenko, Acetylene catalytic hydrochlorination over mechanically pre-activated K_2PdCl_4 salt: a study of the reaction mechanism, J. Catal. 288 (2012) 33–43.
[28] W. Tang, E. Sanville, G. Henkelman, A grid-based Bader analysis algorithm without lattice bias, J. Phys. Condens. Matter 21 (2009).
[29] S.K. Xing, G.C. Wang, Reaction mechanism of ethanol decomposition on Mo_2C(100) investigated by the first principles study, J. Mol. Catal. A Chem. 377 (2013) 180–189.
[30] R.I. Masel, Principles of Adsorption and Reaction on Solid Surfaces, John Wiley & Sons, 1996, p. 513.